PNAS

Supplementary Information for

FLASH X-ray spares intestinal crypts from pyroptosis initiated by cGAS-STING activation upon radioimmunotherapy

Xiaolin Shi, Yiwei Yang, Wei Zhang, Jianxin Wang, Dexin Xiao, Huangge Ren, Tingting Wang, Feng Gao, Zhen Liu, Kui Zhou, Peng Li, Zheng Zhou, Peng Zhang, Xuming Shen, Yu Liu, Jianheng Zhao, Zhongmin Wang, Fenju Liu, Chunlin Shao, Dai Wu*, Haowen Zhang*

Corresponding authors: Dai Wu and Haowen Zhang
Email: wudai04@caep.cn (D.W.); hwzhang@suda.edu.cn (H.Z.)

This PDF file includes:

Materials and Methods

Conventional irradiation

For WAI, an X-RAD 320iX Biological Irradiator (Precision X-ray, North Branford, CT, USA) was used at a dose rate of 1.6 Gy/min. A radiation field extended 30 mm from the pubic symphysis to the xiphoid process while the other body areas of mice were shielded by lead. CONV RT was performed by the Pxi SmART RAD system (Precision X-ray, North Branford, CT, USA). *In-vitro* studies were performed via 160-kV X-ray at a dose rate of 1.18 Gy/min by a biological research irradiator (Rad Source, RS-2000 Pro, Buford, GA, USA). Detailed characters of the X-ray generators for CONV irradiation were listed in Table S1.

FLASH Setup

The FLASH irradiation was carried out using the platform for advanced RT research (PARTER) at the Chengdu THz Free Electron Laser facility (CTFEL) in China. The electron beam, generated by a laser-driven cathode, was accelerated to 6 MeV and then bombarded a Tungsten target to produce bremsstrahlung X-rays. The beam current was controlled by adjusting the driving laser. The delivered mean dose rate in this study was 110-120 Gy/s (instantaneous dose rate ≈ 1.85×10^5 Gy/s), while the total given dose was set by regulating the width of the macro-pulse.

A 6-mm–thick stainless-steel primary collimator was mounted at 14 mm downstream of the target and a 50-mm–thick lead secondary collimator was mounted close upstream of the sample. The collimation hole on the secondary collimator was designed and processed before irradiation according to different field sizes and SSDs.

The electron beam was monitored in real-time by a fast current transformer (Bergoz, ict-082-012-05, Saint-Genis-Pouilly, France) installed upstream of the target. The X-ray was monitored by a diamond detector (Cividec, B3, Vienna, Austria) installed at the entrance of the collimator. The signal was sent through a coaxial cable to an oscilloscope (Rigol, DS7034, Beijing, China) for digitalization. This oscilloscope could automatedly capture, store and integrate these transient pulses. The integration given by the oscilloscope was used as a monitor unit to measure the machine output from the accelerator.

The determination of the irradiation fields of FLASH WAI and FLASH RT

The procedure to determine the aperture size of the collimator (27 × 27 mm^2) and the corresponding irradiation field (30 × 30 mm^2) in FLASH WAI was as follows: (i) Determining the size of the aperture in the collimator. Considering that the collimator could not be adjusted online, the aperture size was determined in advance by calculation according to the point-source assumption and the geometry of the platform (SSD, position of the collimator, and thickness of the mice). This was a general method for aperture design, and the aperture size was set to 27 × 27 mm^2 for a 30 × 30 mm^2 abdominal radiation field. (ii) Adjusting the mean dose. After the collimator was mounted on the platform, the absolute dose and dose distribution were measured using an EBT3 film sandwiched by 8-mm solid water phantoms. The mean dose in the 30 × 30 mm^2 region given by analyzing the EBT3 film was associated with the beam monitor units. Next, the beam current was adjusted till the monitor units revealed a mean dose reaching the target value, and the mean dose and dose distribution were checked again using an EBT3 film. At this point, the size of the region in which the mean dose equal to the target dose was defined as the field size (30 × 30 mm^2) in this study.

Accordingly, FLASH RT was accomplished with a 50-mm–thick lead collimator with an aperture size of 18 × 18 mm^2 to obtain a 20 × 20 mm^2 radiation field.

Dosimetry of FLASH X-ray irradiation

The dosimetry system of FLASH irradiation included a passive dosimeter and an active dosimeter. A dose rate independent Gafchromic™ EBT3 radiochromic film (Ashland Inc., Covington, KY, USA) was used as a passive dosimeter. The EBT3 film was calibrated using a 6-MV clinical linac ELEKTA Precise (Elekta AB, Stockholm, Sweden) and a farmer ionization chamber FC-65G (IBA Dosimetry GmbH, No.1463, Schwarzenbruck, Germany) associated with an electrometer (IBA Dosimetry GmbH, Dose1, Schwarzenbruck, Germany). The RGB value of the EBT3 films was scanned using Epson Expression 12000XL (Seiko Epson Corporation, Japan) 24 h after irradiation and analyzed by codes written using Matlab® 2009 software (MathWorks, USA). The active dosimeter contained a pinpoint ionization chamber (PTW, Ref. 31022, Germany) and an electrometer (PTW, UNIDOS-Webline, Germany) working in integration mode. The passive dosimeter was compared with the active dosimeter at the same FLASH irradiation condition.

Calculation of X-ray spectra and PDD curves

The spectra of 160- to 320-kV X-ray generators and FLASH X-ray generator were given by Geant4 Monte-Carlo simulation, while the spectrum of 6-MV CONV clinical linac was given by Electron Gamma Shower (EGS) computer code system.

The PDD curve of FLASH X-ray irradiation was measured by EBT3 films mounted in solid water phantoms. Whereas the PDD curves in CONV irradiations, including 160 kV, 225 kV, 320 kV, and 6 MV, were obtained by GEANT4 simulation or by referring datasheet of the corresponding machine.

Mice and cell line

C57BL/6 mice were obtained from the Shanghai SLAC laboratory animal Co., Ltd. The PD-L1 KO mice with the C57BL/6 background were purchased from Shanghai Model Organisms Center, Inc. Genotyping was performed following the protocols of Jackson Laboratory. Male mice were subjected to IR exposure at 8 to 10 wk of age. The study was conducted in compliance with local animal welfare laws and policies. All procedures were approved by the ethics committee of Soochow University.

Mouse colon carcinoma MC38 cells and human intestinal epithelial cell line HIEC-6 cells were purchased from ATCC and cultured at 37℃ in an incubator containing 5% CO_2. MC38 cells were cultured in RPMI-1640 medium supplied with 10% fetal bovine serum, penicillin (100 U/ml), and streptomycin (100 μg/ml). HIEC-6 cells were cultured in OptiMEM 1 Reduced Serum Medium (Gibco, no. 31985), supplied with 4% fetal bovine serum, 20 mM HEPES (Gibco, no. 15630080), 10 mM L-Glutamine (Gibco, no. 25030081), 10 ng/mL EGF (Peprotech, no. AF-100-15).

Intestinal crypt isolation

Mouse small intestine was cut longitudinally and flushed with ice-cold PBS. The villi were collected by scraping the intestine with a glass coverslip and stored for further protein analysis. The remaining small intestine was cut into small pieces and incubated in PBS with 2 mM EDTA for 30 min at 4℃ with continuous shaking. After incubation, the tissue fragments were separated by vigorous shaking. The supernatant enriched with crypts was passed through a 70-μm cell strainer (BD Falcon, no. 352350). After centrifugation, the final fraction of intestinal crypts was used for Western blot analysis or further culture.

Organoid culture and irradiation

Small intestinal crypts were cultured as previously described (1). Briefly, isolated crypts were suspended with Matrigel (Corning, no. 356231) and incubated with advanced DMEM/F12 medium (Thermo Fisher Scientific, no. 12634-010) which was supplemented with EGF (Peprotech, no. 315-09-100), Noggin (Peprotech, no. 250-38-5), R-spondin (Peprotech, no. 315-32-5), N2 (Thermo Fisher Scientific, no. 17502048), B27 (Thermo Fisher Scientific, no. 17504044), and Y-27632 dihydrochloride monohydrate (Sigma, no. Y0503) in 24-well plates. Plates were maintained at 37℃ in an incubator containing 5% CO_2.

After being cultured for 2 days *in vitro*, organoids were exposed to CONV or FLASH irradiation at different doses, and percentages of surviving organoids were calculated 6 days post-IR. Live and dead organoids were defined as previously described (2).

Immunoblotting

Tissue homogenates were lysed in radioimmunoprecipitation assay (RIPA) buffer (Thermo Fisher Scientific, no. 89900) supplemented with a protease inhibitor cocktail (Bimake, no. B14001). Proteins were separated by SDS-polyacrylamide gel electrophoresis and transferred onto polyvinylidene fluoride membranes (Millipore, no. ISEQ00010). The membranes were immunoblotted with primary antibodies and proteins were detected with HRP-conjugated secondary antibodies. Immunoreactivity was visualized by FluorChem M (ProteinSimple, San Jose, CA, USA). The following primary antibodies were used: anti–PD-L1 (Abcam, no. ab213480), anti–Caspase-3 (CST, no. 9662), anti-GSDME (Abcam, no. ab215191), anti-Granzyme B (Abcam, no. ab255598), anti-STING (CST, no. 50494), anti–phospho-STING (Ser365) (CST, no. 72971), anti–TBK-1 (CST, no. 3504), anti–phospho-TBK-1 (Ser172) (CST, no. 5483), anti–IRF-3 (CST, no. 4302), anti–phospho-IRF3 (Ser396) (CST, no. 4947S), anti–γ-H2AX (phospho Ser139) (Abcam, no. ab81299), anti–phospho-53BP1 (Ser25) (Abcam, no. ab70323), anti–TREX-1 (Santa Cruz, no. sc-133112), anti-GFP (Beyotime Inc, no. AG279, Shanghai, China), anti–β-actin (Abcam, no. ab8226). The

protein level was determined from the immunoblot quantification using the Image J software (V1.53c, National Institutes of Health, Bethesda, MD, USA).

Gut permeability detection

On day 0, 3, and 7 after IR exposure, mice were fasted for 4 h and was given 50 mg per 100 g body weight of FITC-dextran (4 kD) (Sigma, no. 46944) by gavage in a volume of 0.2 ml. Mouse peripheral blood was collected at 4 h after the administration of FITC-dextran. The fluorescence intensity of serum samples was measured using a multifunctional microplate reader (BioTek, Synergy NEO, VT, USA).

H&E, IHC, and Masson staining

Small intestines of mice were harvested and fixed in 10% neutral-buffered formalin overnight, embedded with paraffin, and then cut into 5-μm sections. Slides were stained with H&E. The number of crypts per millimeter and the thickness of epithelium were quantified. For the IHC staining, sections were incubated with anti-Ki67 (Abcam, no. ab16667; 1:50) at 4℃ overnight. After incubating with a secondary antibody for 1 h at room temperature, sections were stained by DAB (Zhongshan Golden Bridge Biotechnology Co., Ltd., no. ZLI-9018, Beijing, China), and counterstained with hematoxylin. The number of Ki67-positive crypts and Ki67-positive cells in the crypt was measured. Masson staining was performed with Masson's trichrome staining kit (Solarbio Life Sciences, no. G1340, Beijing, China) following the manufacturer's protocol. Images were captured with an OLYMPUS microscope (IX73, TKY, Japan), while measurements of the collagen volume fraction were performed using Image J software (V1.53c, National Institutes of Health, Bethesda, MD, USA).

Immunofluorescence

At indicated time points after 4-Gy irradiation, HIEC-6 cells were fixed with 4% paraformaldehyde for 10 minutes and permeabilized with 0.2% Triton X-100 for 10 min at room temperature. After permeabilization, samples were blocked in 5% BSA for 60 minutes at room temperature, and incubated at 4℃ overnight with an anti-53BP1 antibody (Abcam, no. ab175933, 1:100). Secondary antibody was incubated (1:500) at the following day. After samples were mounted with Mounting Medium with DAPI (Abcam, no. ab104139), 53BP1 foci were detected by an OLYMPUS microscope (FV1200, TKY, Japan).

Flow cytometry analysis

Before undergoing flow cytometry analysis, intestinal crypts and tumors were harvested and processed into single-cell suspensions with Accutase (Thermo Fisher Scientific, no. A1110501). The dissociated cells were stained with the specific surface marker antibodies, anti–CD3-APC (Biolegend, no. 100236), and anti–CD8-PE (Biolegend, no. 100707) in PBS with 2% BSA for 30 min at 4℃. Isotype controls were applied for gating, while single-stain samples were utilized for the proper compensation of flow cytometry channels. Samples were analyzed by BD FACS flow cytometer (Becton, Dickinson and Company, Canto II, Franklin Lakes, NJ, USA), and data were analyzed using Flowjo software (Version 7.6.1, TreeStar, Ashland, OR, USA).

FTY-720 administration

Mice received FTY-720 (Selleck, no. S5002) one day before WAI by intraperitoneal injection at a dose of 25 μg per mouse, and were treated with FTY-720 (5 μg/mouse/day) for consecutive days as described previously (3, 4) until sacrifice.

AAV transfection

GSDME knockdown (AAV-sh *Gsdme*-EGFP) and control (AAV-sh scramble-EGFP) recombinant adeno-associated virus vectors 9 were purchased (GENECHEM Biotech, Shanghai, China) and injected into PD-L1 KO mice through tail vein (5×10^{11} physical particles per mouse). Thirty days after transfection, mice were subjected to CONV X-ray WAI and the expression levels of GFP within frozen sections of small intestines were detected by an OLYMPUS microscope (FV1200, TKY, Japan) on day 3 post-IR.

Analysis of single-cell RNA-seq data

The single-cell RNA-seq data (10 × Genomics data, GEO accession number: GSE117783) (5) deposited in the GEO database were downloaded from https://www.ncbi.nlm.nih.gov/geo/query/acc.cgi?acc=GSE117783 and processed with Seurat's

standard process (Version 4.1.2) as described previously (6). Using straightforward analysis, cells with high *Cd3e* and *Cd8a* expression were classified as $CD8^+$ T cell subpopulations.

qRT-PCR

Total RNA of intestinal crypts was extracted by DNA/RNA/Protein kit (Omega, no. R6734-01) and was reverse-transcribed to cDNA with RT Master Mix (TAKARA, no. RR036A) following the manufacturer's protocol. cDNA samples were further amplified by a fast real-time PCR system of Applied Biosystems (Life Technologies, ViiA7, Carlsbad, CA, USA) using the SYBR green PCR kit (Qiagen, no. 208056) according to the manufacturer's instructions. The following primers were used (5' to 3'): *Ccl5*: forward, CACCACTCCCTGCTGCTT; reverse, ACACTTGGCGGTTCCTTC; *Cxcl9*: forward, TTTTGGGCATCATCTTCCTGG; reverse, GAGGTCTTTGAGGGATTTGTAGTGG; *Cxcl10*: forward, CTTCTGAAAGGTGACCAGCC; reverse, GTCGCACCTCCACATAGCTT; *Cxcl11*: forward, AACAGGAAGGTCACAGCCATAGC; reverse, TTTGTCGCAGCCGTTACTCG; *Ifnb1*: forward, GGTGGAATGAGACTATTGTTG; reverse, AGGACATCTCCCACGTC; *Gapdh*: forward, CTCATGACCACAGTCCATGC; reverse, CACATTGGGGGTAGGAACAC

diABZI administration

For activating STING in PD-L1–deficient mice undergoing FLASH WAI at a single dose of 13 Gy, diABZI (Selleck, no. S8796) was intraperitoneally injected into mice immediately after irradiation at a dose of 2 mg/kg. For activating STING in C57BL/6 mice exposed to fractionated FLASH irradiation (5 Gy at a time in consecutive 5 days, 25 Gy in total, *i.e.*, 5 Gy × 5), diABZI was injected immediately after each fraction at a dose of 1 mg/kg. An anti-mouse PD-L1 antibody was administered immediately after the first fraction of FLASH irradiation at a dose of 10 mg/kg and was injected every two days at the same time point for a total of four times. Small intestines were examined on day 3 after the last IR fraction.

RU.521 treatment

To inhibit the cGAS activity, C57BL/6 mice were intraperitoneally injected with RU.521 (Selleck, no. S6841) at a dose of 10 mg/kg at 12 h before each fraction of CONV or FLASH WAI (5 Gy × 5). An anti-mouse PD-L1 antibody was administered immediately after the first fraction of irradiation at a dose of 10 mg/kg and was injected every two days at the same time point for a total of four times. Small intestines were examined on day 3 after the last IR fraction.

Cytoplasmic dsDNA quantification

Organoids or MC38 tumor cells were irradiated by 8-Gy of CONV or FLASH X-ray *in vitro*. The cytoplasm was extracted using a Mitochondria Isolation Kit (Thermo Fisher Scientific, no. 89874). Cytoplasmic dsDNA was quantified using the Quant-iT PicoGreen dsDNA Assay Kit (Thermo Fisher Scientific, no. P11496). The fluorescence intensity was detected by a multifunctional microplate reader (BioTek, Synergy NEO, VT, USA) and was normalized by the protein concentration of the cytoplasmic fraction.

Cytosolic dsDNA Staining

MC38 cells were exposed to 8-Gy CONV or FLASH irradiation and were incubated with pre-warmed culture media containing PicoGreen (200-fold dilution) (Thermo Fisher Scientific, no. P11496) and MitoTracker (100 nM) (Thermo Fisher Scientific, no. M7512) 9 h post-IR for 1 h to stain cytosolic dsDNA and mitochondria, respectively. Before DAPI (Abcam, no. ab104139) staining, cells were fixed with 3.7% formaldehyde in culture media for 15 min. The fluorescence was detected by an OLYMPUS microscope (FV1200, TKY, Japan).

Tumor radioimmunotherapy

Male C57BL/6 mice were subcutaneously inoculated with 5×10^5 MC38 cells on the left flanks (primary tumor) on day 0 and the right flanks (secondary tumor) 3 days later. Ten days after implanting primary tumors, mice were randomly assigned into different groups based on tumor volumes and subjected to RT with different radiation modalities for 5 Gy at a time for consecutive 5 days (5 Gy × 5). CONV RT was performed by the Pxi SmART RAD system using a 20 × 20 mm^2 square collimator according to the treatment plan calculated by the software SmART Plan. FLASH RT was accomplished with a 50-mm–thick lead secondary collimator at the PARTER platform of CTFEL to obtain a 20 × 20 mm^2 radiation field. Mice were intraperitoneally injected with anti-mouse

PD-L1 monoclonal antibody (Bio X Cell, clone 10F.9G2) at a dose of 10 mg/kg on day 10 after the primary tumor was implanted, and was injected every two days for a total of four times. For radioimmunotherapy, an anti-mouse PD-L1 antibody was administered immediately after the first fraction of RT and was injected every two days at the same time point for a total of four times. Tumor volumes were evaluated every two days with a digital caliper and were calculated using the following formula (V = longest dimension × perpendicular dimension × perpendicular dimension × 0.5) as previously described (4). Mice with tumors greater than 15 mm in diameter or 2000 mm^3 in volume were euthanized by CO_2 asphyxiation.

Statistical analysis

Sample sizes were chosen based on pilot experiments and empirically to ensure adequate statistical power. Graph generation and statistical analysis were performed with GraphPad Prism (version 8.0.2) (GraphPad Software Inc., San Diego, CA, USA) and SigmaPlot (version 10.0) (Systat Software Inc. San Jose, CA, USA). Each experiment was repeated independently at least two times with similar results, and quantitative data were presented as the mean ± SEM. Statistical significance was determined using a two-tailed Student's *t*-test. Survival between groups was compared using the Kaplan–Meier method with the log-rank test.

Figure S1

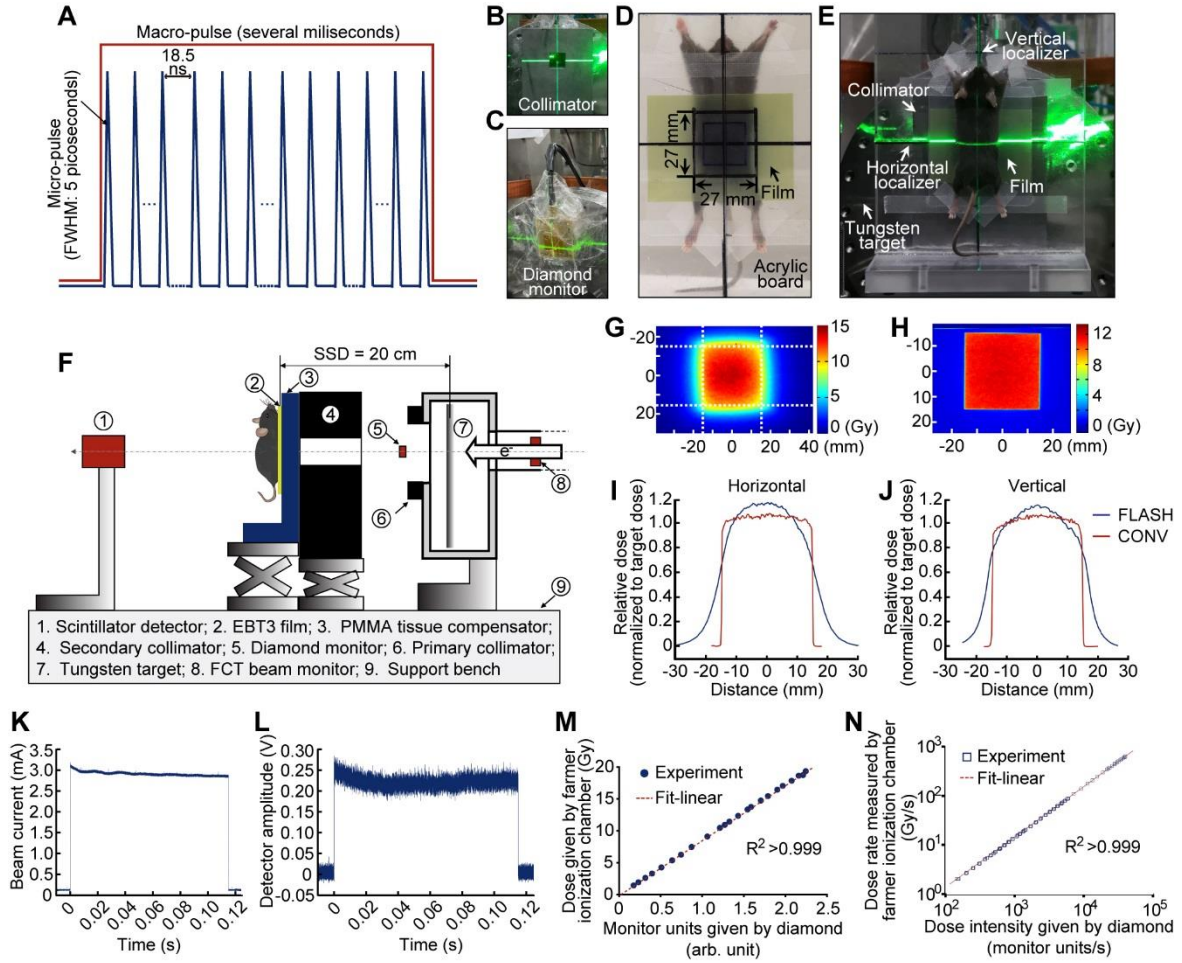

Fig. S1. Parameters and dosimetry of the FLASH and CONV X-ray WAI. (*A*) Pulse structure of the electron beam from the superconductor accelerator at CTFEL. (*B*) A lead secondary collimator with an aperture of 27 × 27 mm^2 was used to delimitate the FLASH irradiation field. (*C*) The diamond monitor was mounted upstream of the secondary collimator. (*D*) A 15-mm**–**thick polymethyl methacrylate (PMMA) plate was used for dose build-up and mice fixing, and an EBT3 film was placed between the PMMA plate and the anterior surface of the irradiated mouse for dose evaluation. (*E*) Laser lines were applied for positioning. (*F*) The schematic diagram of the *in-vivo* FLASH X-ray experiment. (*G* and *H*) The corresponding FLASH (*G*) or 320-kV CONV (*H*) dose distribution of an EBT3 film mounted at 8-mm depth in solid water. A 30 × 30 mm^2 FLASH irradiation field is indicated by white dotted lines in (*G*). (*I* and *J*) The horizontal (*I*), as well as the vertical (*J*) dose profiles, represent the dose distribution in (*G* and *H*). (*K* and *L*) A representative beam current curve in a 115 ms macro-pulse (*K*) and an amplitude curve of the diamond detector (*L*) are presented. (*M* and *N*) The ionization chamber was mounted at 8-mm depth in solid water to measure the curve of the 'dose-monitor unit' (*M*) and 'dose rate-monitor unit/s' (*N*).

Figure S2

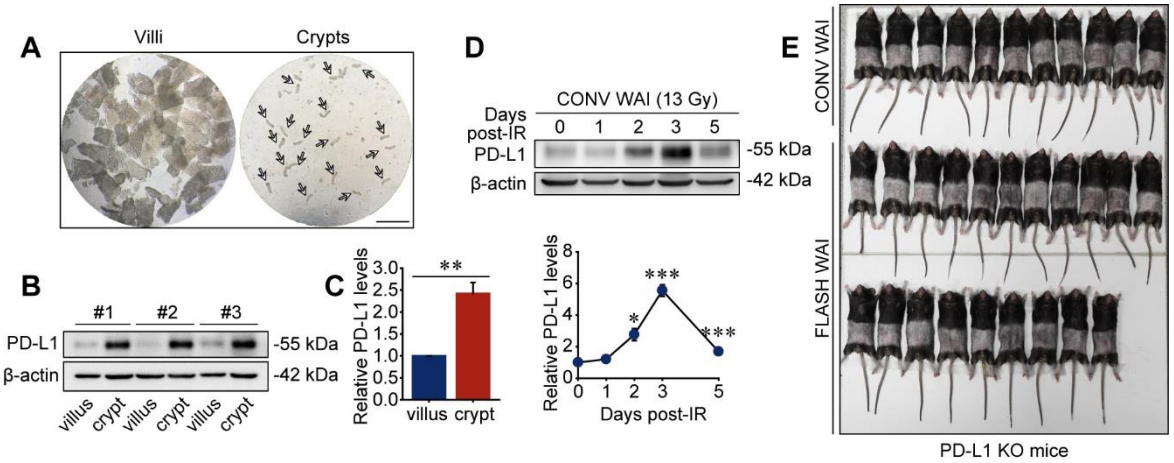

Fig. S2. The spatial and temporal expression of PD-L1 in mouse small intestines post-IR. (*A*–*C*) Villi and crypts were isolated from untreated small intestines of C57BL/6 mice, and the expression levels of PD-L1 and β-actin (internal control) were determined by Western blotting analysis. Hollow arrows denote isolated intestinal crypts (*A*). The Immunoblot pictures are shown (*B*). The relative ratio of PD-L1 to β-actin of villi and crypts was determined from the immunoblot quantification using the Image J software and normalized to expression levels of villi (*C*). (*D*) Western blot analysis of PD-L1 and β-actin expression levels in mouse intestinal crypts at the indicated time after 13-Gy CONV WAI. The relative ratio of PD-L1 to β-actin was normalized to the control group. (*E*) Hair depigmentation of PD-L1 KO mice at 6 months after 13-Gy CONV or FLASH WAI. Data are pooled from three (*D*) independent experiments. Error bars indicate SEM. **P* < 0.05, ***P* < 0.01, and ****P* < 0.001 were determined by a two-sided Student's *t*-test.

Figure S3

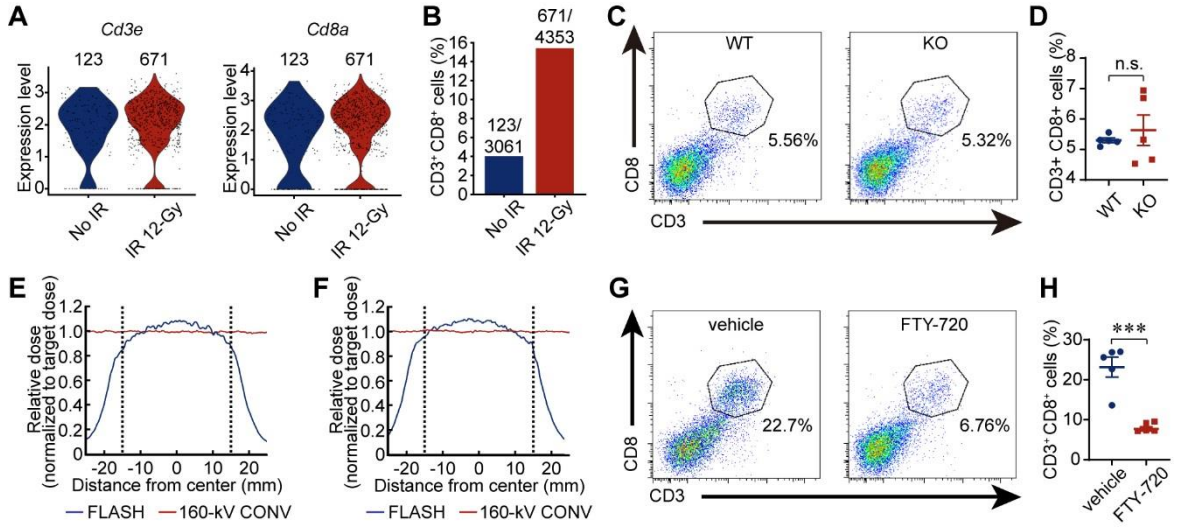

Fig. S3. The proportion of CD8⁺ T cells in the intestinal crypts. (*A*) Violin plots show the expression levels of *Cd3e* (left) and *Cd8a* (right) of $CD3^+CD8^+$ T cells in intestinal crypts under indicated treatments. Data were normalized by Seurat's Log Normalize method, and the numbers of $CD3^+CD8^+$ T cells are indicated. (*B*) Percentages of $CD3^+CD8^+$ T cells were defined by high expression levels of *Cd3e* and *Cd8a*. The fractions indicate the proportions of $CD3^+CD8^+$ T cells in the intestinal crypts under indicated treatments. (*C* and *D*) Flow cytometric analysis of $CD3^+CD8^+$ cells in the intestinal crypts from mice left untreated. Data are presented as representative plots (*C*) and quantified percentages (*D*) (n = 5 mice per group). (*E* and *F*) The spatial dose distribution of X-rays in the form of horizontal (*E*) and vertical (*F*) profiles is shown. The intestinal organoid samples were placed in the center of the area indicated by the black dotted lines. (*G* and *H*) PD-L1–deficient mice were dosed with an intraperitoneal injection of FTY-720 (25 μg/mouse) 1 day before 13-Gy CONV WAI and were treated with FTY-720 (5 μg/mouse/day) for consecutive days until sacrifice. Crypt-infiltrated $CD3^+CD8^+$ cells of mice at 3 days after WAI were determined by flow cytometric analysis (*G*), and data are presented as quantified percentages (*H*) (n = 5 mice per group). Data are pooled from two independent experiments [(*C* and *D*), (*G* and *H*)]. Error bars indicate SEM. ***$P < 0.001$, and no significance (n.s.) were determined by a two-sided Student's *t*-test.

Figure S4

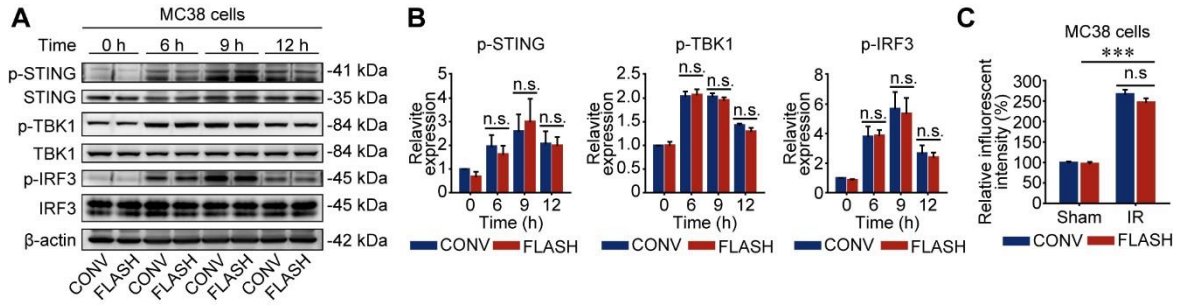

Fig. S4. FLASH and CONV irradiation elicit comparable cytoplasmic dsDNA fragments and cGAS-STING activation in MC38 cells. (*A* and *B*) MC38 cells were irradiated by 8-Gy CONV or FLASH irradiation for Western blot analysis. Representative pictures are shown (*A*). The relative ratio of indicated protein to β-actin was determined and was normalized to the 'CONV 0 h' group (*B*). (*C*) MC38 tumor cells were subjected to 8-Gy X-ray of CONV or FLASH irradiation, and the cytoplasm was extracted 9 h post-IR to quantify the cytosolic dsDNA by detecting the fluorescence intensity of PicoGreen-stained dsDNA. Data are pooled from three independent experiments (*A* and *B*) or represent three independent experiments (*C*). Error bars indicate SEM. ***$P < 0.001$ and n.s. were determined by a two-sided Student's *t*-test.

Figure S5

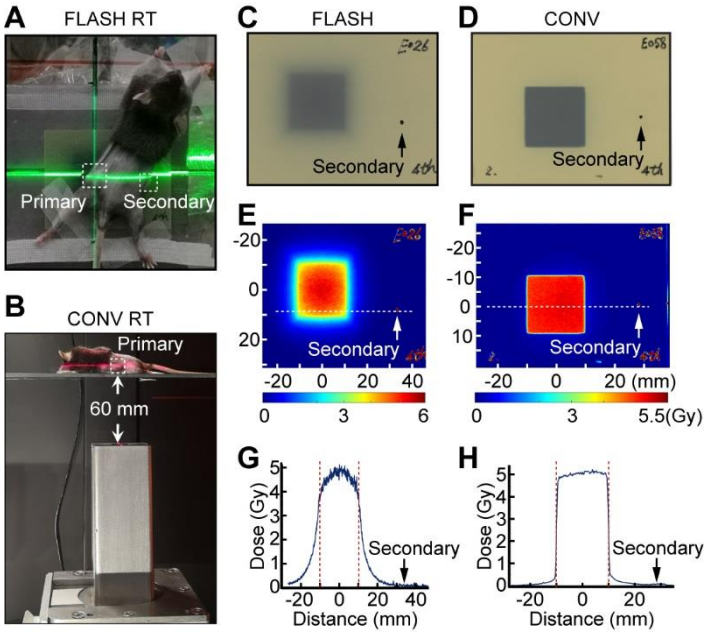

Fig. S5. The positioning and the dose distribution of tumor-bearing mice receiving FLASH or CONV RT. (*A* and *B*) The positioning of the animal exposed to FLASH (*A*) or CONV (*B*) X-ray RT is presented. For FLASH irradiation, a lead secondary collimator was used to delimitate a 20 × 20 mm^2 radiation field. (*C*–*H*) EBT3 films were used for dose evaluation in both CONV and FLASH irradiation. Representative scanned images of monitor films 24 h after FLASH (*C*) and CONV (*D*) irradiation are displayed, while the corresponding dose distribution in FLASH (*E*) and CONV (*F*) irradiation is given. The dose-position curve in (*G*) and (*H*) represents the dose distribution along the white dotted line in (*E*) and (*F*), respectively. Arrows denote the position of the secondary tumor.

Figure S6

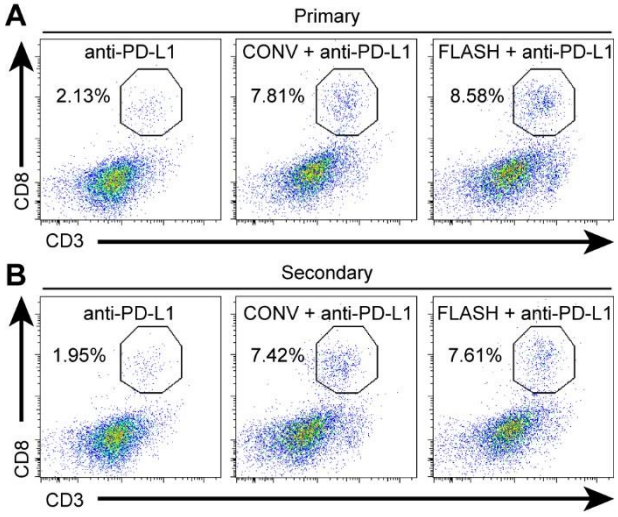

Fig. S6. Flow cytometric analysis of $CD3^+CD8^+$ cells in MC38 tumors. (*A* and *B*) $CD3^+CD8^+$ cells within primary and secondary tumors 5 days after the last injection of anti–PD-L1 antibody were tested by flow cytometric analysis (n = 5 mice per group). Representative plots of $CD3^+CD8^+$ cells in primary (*A*) and secondary (*B*) tumors are shown.

Figure S7

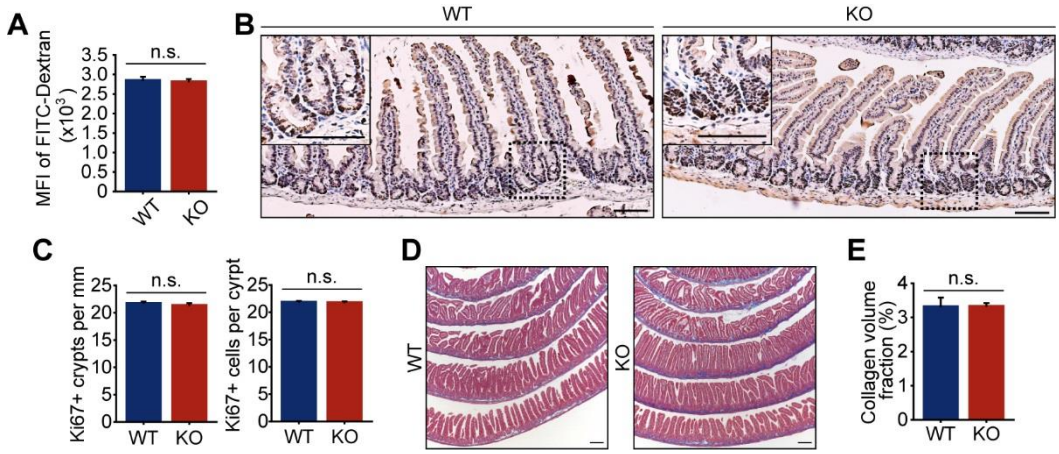

Fig. S7. Intestinal integrity of wildtype and PD-L1 KO mice. (*A*) The gut permeability of mice left untreated was determined by testing the intensity of fluorescence of FITC-dextran (n = 6 mice per group). MFI, mean fluorescence intensity. (*B* and *C*) Representative pictures of Ki67 staining sections of proximal intestines from untreated mice are shown (*B*), and Ki67$^+$ crypts per millimeter, as well as Ki67$^+$ cells per crypt, were quantified (n = 3 mice per group) (*C*). (*D* and *E*) Representative pictures of Masson staining sections of proximal intestines from 8-months–old mice left untreated are shown (*D*), and intestinal fibrosis was quantified by Image J (*E*) (n = 3 mice per group). Data represent three (*A*–*C*) or two (*D* and *E*) independent experiments. Error bars indicate SEM. n.s. was determined by a two-sided Student's *t*-test. Scale bars, 200 μm.

Figure S8

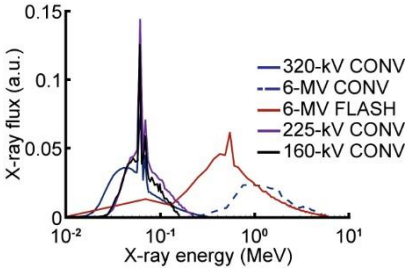

Fig. S8. The energy spectra of the X-ray sources used for FLASH- and CONV- irradiation. The energy spectra of 160- to 320-kV X-ray generators and FLASH X-ray generator were given by Geant4 Monte-Carlo simulation, and the energy spectrum of 6-MV CONV clinical linac was provided by Electron Gamma Shower (EGS) computer code system.

Figure S9

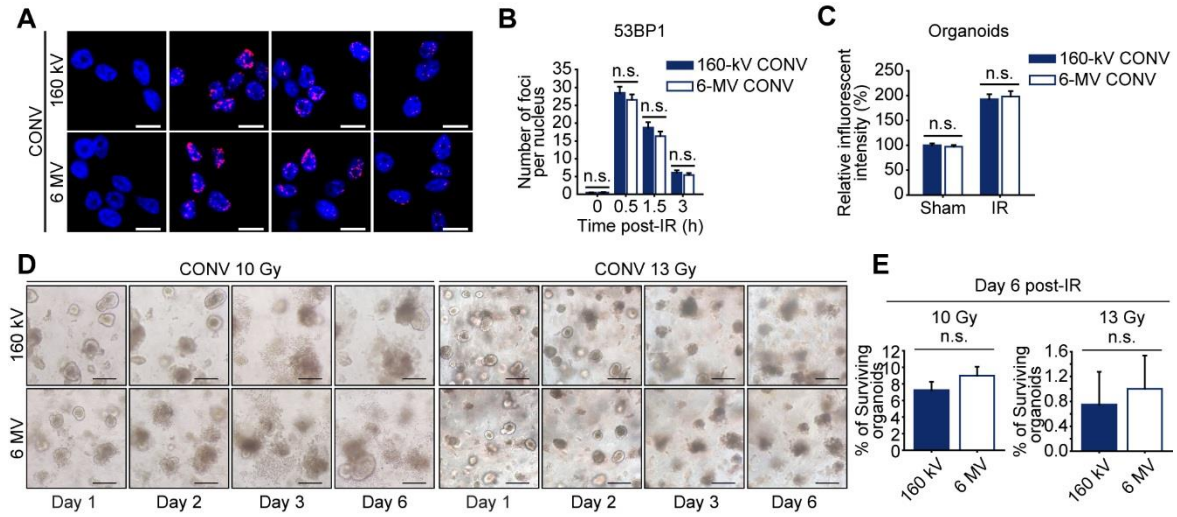

Fig. S9. Damages of HIEC-6 cells and intestinal organoids induced by 160-kV or 6-MV CONV X-ray. (*A*) Representative images of 53BP1 fluorescent staining in nuclei of HIEC-6 cells exposed to 4-Gy 160-kV or 6-MV CONV X-ray. Scale bars, 10 μm. (*B*) Quantification of nuclear 53BP1 foci. (*C*) Organoids derived from isolated intestinal crypts of PD-L1 KO mice were subjected to 8-Gy 160-kV or 6-MV CONV X-ray irradiation, and the cytoplasm was extracted 9 h post-IR to quantify the cytosolic dsDNA by detecting the fluorescence intensity of PicoGreen-stained dsDNA. (*D* and *E*) Organoids derived from isolated intestinal crypts of PD-L1 KO mice were subjected to 10- or 13-Gy CONV X-ray irradiation. Representative pictures of the same microscopic fields at the indicated time post-IR are displayed. Scale bars, 200 μm (*D*). The percentages of surviving organoids (intact/refractive) were calculated on day 6 after irradiation (*E*). Data represent three independent experiments (*A*–*E*). Error bars indicate SEM. n.s. was determined by a two-sided Student's *t*-test.

Figure S10

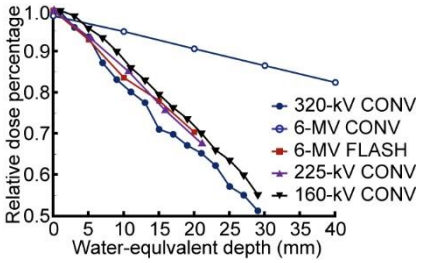

Fig. S10. The PDD curves of the X-ray sources used for FLASH- and CONV- irradiation. The PDD curve of FLASH X-ray irradiation was measured by EBT3 films mounted in solid water phantoms. Whereas the PDD curves in CONV irradiations, including 160 kV, 225 kV, 320 kV, and 6 MV, were obtained by GEANT4 simulation or by referring datasheet of the corresponding machine.

Figure S11

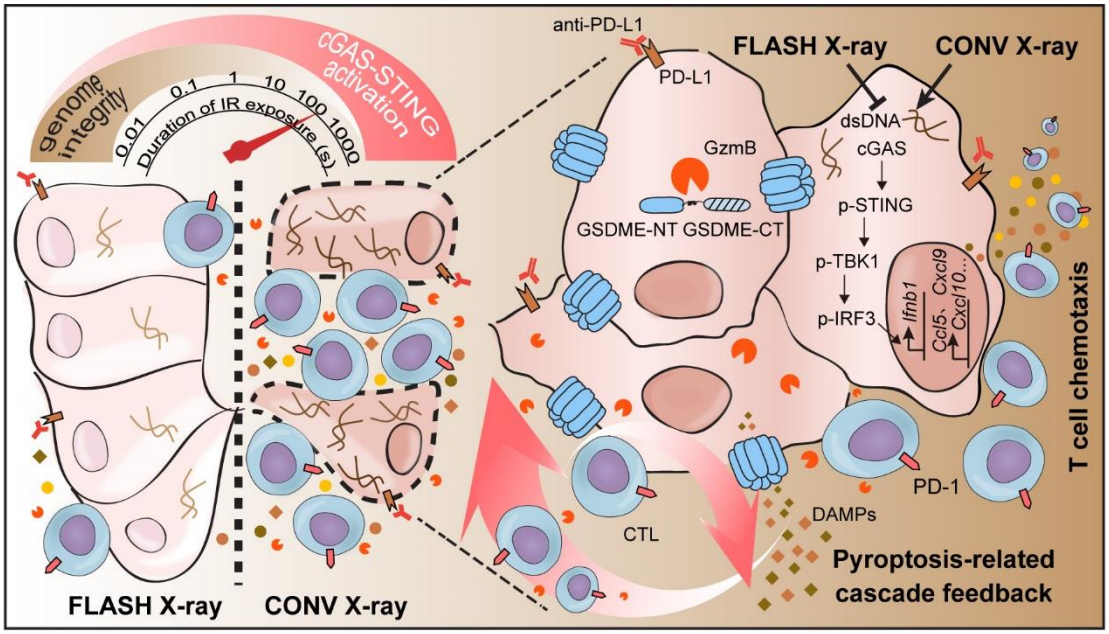

Fig. S11. The 'DNA integrity' hypothesis in the 'FLASH effect'. The 'relatively intact DNA integrity' within intestinal cells during the 'instantaneous' IR exposure is the critical molecular machinery of FLASH X-ray in eliciting less cGAS-STING activation than CONV IR and in impeding the cascade feedback comprising CTL infiltration and lethal intestinal pyroptosis upon radioimmunotherapy.

Table S1. Key characters of the X-ray generators for CONV irradiation.

X-ray generator	Energy	Filter	Used for	SSD[1]	Collimation	Collimator-animal distance	Radiation field size for animal experiments	Beam Monitoring	Tool and frequency for dosimetry calibration
X-RAD 320i	320 kV	2 mm Al	WAI[2] (*in vivo*)	50 cm	Inherent adjustable X-ray beam collimator and additional 1-cm–thick lead collimator	< 1 cm between mice and the secondary collimator	3.0 × 3.0 cm^2	PTW 7862 parallel plate transmission chamber	ACCU-Dose+ Digitizer Module (Radcal, California, USA) with a gold standard ACCU-Dose ion chamber (10X6-0.18); Once a year. Rechecked before mice irradiation using EBT3.
SIEMENS Primus-H	6 MV	Low–melting-point lead (LML)	Organoids HIEC-6 cells (*in vitro*)	100 cm	Inherent primary collimator, Multi-Leaf Collimator (MLC)	–	–	Inherent parallel plate transmission chamber	Farmer ionization chamber FC65-G (IBA Dosimetry GmbH, No. 1463) associated with an IBA DOSE1TM electrometer; Once a week.
XRAD-SmART	225 kV	0.3 mm Cu	Tumor radiotherapy (*in vivo*)	30 cm	Inherent collimator of 143.9 mm in length with square aperture (#S20)	6 cm between mice and the secondary collimator	2.0 × 2.0 cm^2	Inherent treatment planning system SmART-Plan	ACCU-Dose+ Digitizer Module (Radcal, California, USA) with a gold standard ACCU-Dose ion chamber (10X6-0.18); Once a year. Rechecked before mice irradiation using EBT3.
RS-2000 Pro	160 kV	0.3 mm Cu	Organoids HIEC-6 cells MC38 cells (*in vitro*)	53 cm	No additional collimator except the built-in window of the X-ray tube	–	–	No monitor	ACCU-Dose+ Digitizer Module (Radcal, California, USA) with a gold standard ACCU-Dose ion chamber (10X6-0.18); Once a year.

1. source–surface distance. 2. whole abdominal irradiation.

References

1. F. Chen *et al.*, TIGAR/AP-1 axis accelerates the division of Lgr5(-) reserve intestinal stem cells to reestablish intestinal architecture after lethal radiation. *Cell Death Dis* **11**, 501 (2020).
2. B. Hu *et al.*, The DNA-sensing AIM2 inflammasome controls radiation-induced cell death and tissue injury. *Science* **354**, 765-768 (2016).
3. S. J. Dovedi *et al.*, Fractionated Radiation Therapy Stimulates Antitumor Immunity Mediated by Both Resident and Infiltrating Polyclonal T-cell Populations when Combined with PD-1 Blockade. *Clin Cancer Res* **23**, 5514-5526 (2017).
4. J. Wei *et al.*, Sequence of alphaPD-1 relative to local tumor irradiation determines the induction of abscopal antitumor immune responses. *Sci Immunol* **6** (2021).
5. A. Ayyaz *et al.*, Single-cell transcriptomes of the regenerating intestine reveal a revival stem cell. *Nature* **569**, 121-125 (2019).
6. Y. Hao *et al.*, Integrated analysis of multimodal single-cell data. *Cell* **184**, 3573-3587 e3529 (2021).